A novel excitation-emission wavelength model to facilitate the diagnosis of urinary bladder diseases

Ilya Rafailov*[1], Scott Palmer[1], Karina Litvinova[1], Victor Dremin[2], Andrey Dunaev[2], Ghulam Nabi[1]

[1] Department of Imaging and Technology, School of Medicine, University of Dundee, Dundee, DD1 9SY, UK

[2] Biomedical Photonics Instrumentation Group, Scientific-Educational Centre of "Biomedical Engineering", State University – Education-Science-Production Complex, Oryol, 302020, Russia

ABSTRACT

Diseases of urinary bladder are a common healthcare problem world over. Diagnostic precision and predicting response to treatment are major issues. This study aims to create an optical cross-sectionional model of a bladder, capable of visually representing the passage of photons through the tissue layers. The absorption, transmission and reflectance data, along with the derived transmission coefficients (of scattering and absorption) were obtained from literature analysis and were used in the creation of a "generic" cross-section optical property model simulating the passage of thousands of photons through the tissue at different wavelengths. Fluorescence spectra of diagnostically relevant biomarkers excited by the UV and blue wavelengths were modelled on the basis of the Monte-Carlo method. Further to this, fluorescence data gathered by the "LAKK-M" system from pig bladders was applied to the model for a specific representation of the photon passage through the tissues. The ultimate goal of this study is to employ this model to simulate the effects of different laser wavelength and energy inputs to bladder tissue and to determine the effectiveness of potential photonics based devices for the diagnosis of bladder pathologies. The model will aid in observing differences between healthy and pathological bladder tissues registered by photonics based devices.

Keywords: bladder cancer, non-invasive diagnostics, fluorescence spectroscopy, modelling, Monte Carlo simulation

* i.rafailov@dundee.ac.uk; phone +44(0)1382 660111; medicine.dundee.ac.uk/medical-research-institute/divisions/division-imaging-technology

Photonic Therapeutics and Diagnostics XI, edited by Bernard Choi, et al., Proc. of SPIE
Vol. 9303, 93030W · © 2015 SPIE · CCC code: 1605-7422/15/$18 · doi: 10.1117/12.2077554

1. INTRODUCTION

For years, photonics based techniques have been employed all over the world to screen, diagnose and treat many medical conditions. Their role has been particularly vital for research into various forms of cancer. Of special interest is urinary bladder cancer (BC), which is one of the top ten most prevalent cancers worldwide. Bladder cancer can prove fatal in the case of aggressive muscle invasive and metastatic disease. Even non-muscle invasive disease (accounting for around 70% of cases), which is generally non-fatal, experiences high rates of recurrence and progression, resulting in considerable patient morbidity. The high rates of recurrence and progression associated with bladder cancer

make it the single most expensive cancer to treat on a per-patient basis [1,2]. It is therefore imperative, that bladder cancer is detected early. In contrast to deeper lying organs, such as the liver and kidneys, the bladder is easily accessible trans-urethrally through the use of endoscopes, without the need for complex surgery or laparoscopy. As such, it lends itself well to photonics diagnostics using cystoscopic probes, and has been the focus of numerous advances in minimally invasive diagnosis research over the years [3].

To detect and diagnose BC, the current gold standard employs a combination of cystoscopy and urine cytology, with the transurethral resection of the bladder tumour (TURBT) serving not only a therapeutic purpose, but also to provide additional tissue for diagnostic data and disease staging [4]. White light cystoscopy (WLC) is used to visually detect suspicious areas which are then resected. WLC is a technique which has reliable specificity in that it allows the operator/surgeon to directly survey the tissue, however it suffers from low sensitivity, particularly for CIS [5]. This technique may also not reveal the entire extent of the tumour, resulting in incomplete resection and a high risk of recurrence [6]. Alternative detection techniques rely on the use of photoactive agents such as 5-aminolevulinic acid (5-ALA) or Hexaminolevulinate (HAL) preferentially accumulating in neoplastic tissues. In a process known as photodynamic diagnosis (PDD), these molecules are stimulated by blue light to produce a red fluorescence [7]. This technique provides vastly increases detection sensitivity, but at the cost of a reduced specificity compared to WLC. Use of PDD is known to produce a higher chance of false-positive diagnoses, ultimately leading to unnecessary surgical procedures [8]. Therefore, both WLC and PDD suffer from their own respective limitations. Furthermore, neither technique provides direct evidence of inherent molecular changes within tissue.

Recent advances in biophotonics (improvements to cost, signal to noise ratio and tissue penetration of laser sources) have provided potential new avenues for diagnosis of BC through detection and quantification of endogenous tissue fluorescence without the need for fluorescent dyes [9-11]. Numerous endogenous molecules naturally fluoresce when excited with the appropriate wavelength of light. Analysis of tissue autofluorescence spectra under different excitation wavelengths can therefore provide valuable information on tissue architecture, metabolism and inflammation [12-14]. Among the most diagnostically relevant biomarkers are the mitochondrial cofactors NADH and FAD and the structural protein collagen. NADH and FAD provide information on metabolic changes undertaken by cancer cells, with the optical

redox ratio (NADH/FAD) showing promise in the diagnosis and monitoring of several cancers owing to selective accumulation of NADH in cancer cells [15-17]. Conversely, collagen can often provide a diagnostic signal owing to its reduction in tissue as tumours progress owing to the action of destructive enzymes such as Matrix metalloproteinase 9 [18]. It is proposed that this approach can act as a best of both worlds, providing high sensitivity for the diagnosis of early cancers without having to compromise on specificity. Autofluorescence spectroscopy has already proven itself a worthwhile diagnostic tool for the discrimination of many diseases [19-21] and work is currently underway to reliably characterise the autofluorescence properties of healthy and malignant bladder tissue, both *ex vivo* [22] and *in vivo* [3].

Autofluorescence spectroscopy depends crucially on our ability to understand and deconvolve the interactions between light and tissue. In complex systems such as tissue, analysis is not as simple as providing one incident photon and measuring the emitted fluorescence. Processes such as scattering and non-specific absorption of both incident and emitted light often obscure the signals we obtain from tissue. Scattering and non-specific absorption of photons become significant obstacles the deeper we look into tissue, one of the reasons why it is so difficult to detect early grade bladder tumours and CIS. Needless to say, these processes occur differently in tissues with different optical properties and this must be taken into account when designing diagnostic techniques [23,24]. The urinary bladder is comprised of multiple layers, the most obvious of which are the muscular and mucosal layers. Both of these tissue types can be sub-divided even further, with tissue layers often also interspersed by extracellular matrices and structural proteins. Each layer of bladder tissue has its own unique properties, for instance muscle layers scatter much more light than mucosal layers. The multi-layered environment of the bladder (and most other tissues) therefore dramatically changes the passage and properties of light. Many previous studies in the field of autofluorescence spectroscopy have not taken into account the scattering and absorptive effects of different tissue layers. Many accounts have also suffered from falsely attributing malignancy induced changes in tissue optical properties to absolute increases or decreases in tissue fluorophores. This is especially noticeable when matrix degradation or tissue thickening occurs [25,26].

To address this, the optical properties of tissue from many different animals (such as dogs and pigs) and humans have been characterised [27,28]. Databases have been constructed to include data obtained from bladder tissue as well as a wide variety of others (including adipose, brain and heart). Such databases provide information including the coefficients of absorption, scattering and attenuation of tissues. Tissue models, 3D and otherwise, are also starting to become commonplace to allow researchers to adequately model experiments, interpret results and as initial tests for novel photonics based equipment [29,30]. A number of groups have been involved in the development of 3D bladder models, both physical (optical phantoms) and computer simulated. These are generally based on data acquired using OCT and have provided a wealth of information for the design and improvement of white light cystoscopy and photodynamic diagnosis. To this date, however, the authors know of no reliable optical bladder models for the study of autofluorescence which take into account fluorescence contributions of distinct endogenous fluorophores. Minimally invasive diagnostic systems for the measurement of autofluorescence spectra possess immense potential for the detection of bladder cancer however they require a great deal of metrological support and rigorous characterisation and testing before they can be functionally

employed. Here, we have aimed to design and develop a computer simulated optical 3D bladder model to allow the study of propagation of light of a wide range of wavelengths through bladder tissue. We have utilised extensive literature reviews to calculate the absorption and scattering parameters of bladder tissue and used fluorescence spectroscopy over a range of wavelengths to determine tissue quantum fluorescence yields for distinct fluorophores such as NADH. We suggest that this model can be used for direct comparisons of a host of photonic devices to determine clinical worth. It will also allow the modelling of the effects of bladder cancer progression on the optical properties of bladder tissue, providing diagnostic benchmarks by which to set tumour staging and grading criteria.

2. METHODS

2.1 Literature review

A literature analysis was carried out to obtain coefficients of attenuation, scattering and absorption (μ_t, μ_s and μ_a respectively) of bladder tissue. Search was carried out using PubMed, relying on the following key words: bladder, bladder tissue, optical properties, tissue optical properties, absorption, attenuation, scattering. The optical properties of separate layers of bladder tissue were preferred to whole bladder tissue recordings. Particular priority was given to the properties of the bladder mucous and sub-mucous layers.

2.2 Construction of 3D model

TracePro (Lambda Software) was used for the construction of the model. Two layers were constructed in the software: mucosa (area/volume measurements) and muscle (area/volume measurements) to simulate the core layers within urinary bladder tissue. The simulated source was set at 1mm distance away from the detector (diameter of 0.06mm). This was done to mimic the parameters of the MLNDS "LAKK-M". The quantitative modelling was carried out through the use of the Monte-Carlo methodology. This is currently one of the most commonly used methods for describing the distribution of light through biotissues. The core idea behind the method is to account for instances of absorption and scattering along the entire optical path of a photon through an opaque medium.

For the wavelength range of interest (360 – 610 nm) within tissues, the refractive index n, the scattering coefficient μ_s, the absorption coefficient μ_a and the anisotropy factor g were required. Figure 1 displays the core parameters that determine the optical properties of biotissue and their interconnections [31].

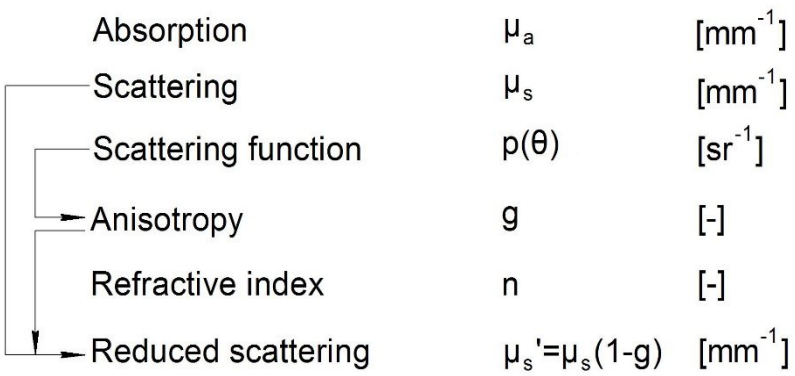

Figure 1. The core optical parameters of biotissue and their interconnection.

During excitation of urinary bladder tissue by light, incident radiation passes through the mucosa and is partially absorbed, exciting the NADH fluorescence. The transmitted component continues towards the muscle layer, where it is further absorbed and diffusely scattered by collagen fibres and other structural components before being passed back through the layers, absorbed and finally received by the detector. The same principles were used to derive the model, with NADH presence in the mucosa simulated using the following criteria [32],[33] and collagen presence using [34],[35] to further maximise the accuracy.

Based on the given parameters, the absorption in biological tissue is taken into account using the Beer-Lambert law:

$$\Phi = \Phi_0 \exp(-\mu_a t), \quad (1)$$

Where Φ and Φ_0 are the missed and incident flux, μ_a is the coefficient of absorption and t is the sample thickness.

To account for the refraction or reflection at the interface of the two layers, Fresnel's law is used. The commonly used Henyey-Greenstein function is used as the scattering phase function:

$$SDF = p(\theta) = \frac{1 - g^2}{4\pi(1 + g^2 - 2g\cos\theta)}, \quad (2)$$

Where g is the anisotropy factor.

The parameter g may have the value between -1 and 1. When g is positive the rays are largely scattered in a forward direction, whereas a negative g will result in a rays scattered in a reverse direction. When g is zero, scattering is isotropic, i.e. equal in all directions.

When the beam passes a scattering medium, it spreads to a random distance x, adjustable using the probability distribution:

$$P(x)dx = \exp(-\mu_s x)dx, \quad (3)$$

Where μ_s is the coefficient of scattering.

When the beam interacts with a material which is thin compared to the mean free path, it passes through that material without scattering. Conversely, if the thickness of the material is large, the beam is highly likely to scatter.

TracePro models fluorescence by using fluorescent properties in conjunction with the material properties of the object constructed and the laws described above. Parameters which can be set include the relative absorption $ab(\lambda)$ and relative excitation $ex(\lambda)$, normalised to the molar extinction coefficient K_{peak} and the relative emission $em(\lambda)$. The concentration of fluorescent material is set by entering the molar concentration C_{molar}. The coefficient of fluorophore absorption in media is determined by:

$$\mu_a(\lambda) = ab(\lambda)K_{peak}C_{molar}, \quad (4)$$

The path length before absorption:

$$d(\lambda) = -\log 10(x)/\mu_a(\lambda), \quad (5)$$

Where x is a random value between 0 and 1.

The number of photons involved in the process, compared to the number of photons previously absorbed by the system, is determined by ascribing quantum efficiency (QE) to the system.

2.3 Fluorescence measurement of urinary bladder tissue

Urinary bladder tissue was obtained as previously described and was split between dome and trigone sections. The bisected bladder was "virtually" divided into 16 sections. Virtual sections of the inner mucosal layer of the bladder were sequentially subjected to optical analysis by the fluorescence spectroscope of a "LAKK-M" multi-functional laser based non-invasive diagnostic device (SPE "LAZMA" Ltd, Russia). The fibre of the device was run along the length of its stand and the probe was placed into direct contact with the bladder tissue. No extra force was applied to the probe. Tissue was scanned sequentially using 4 different excitation sources (UV 365nm, blue 430nm, green 532nm and red 632nm). Five seconds of contact was allocated per wavelength measurement. Resultant tissue fluorescence was recorded across a wavelength range of 300-800nm using an inbuilt spectrometer and processed using custom-made software (LDF 3v3.1.1.403, SPE "LAZMA"). Data was exported and visualised graphically using Origin pro 8 software. The entire procedure was carried out at room temperature, in a windowless dark room to limit noise.

3. RESULTS AND DISCUSSION

3.1 Literature review

The initial stages of the model development required the collation of transmission, reflectance and absorbance properties of bladder tissue. Materials reviewing the optical properties of a selection of different tissues were found [27],[28],[36]. All optical properties of interest obtained from the reviews regarding human tissue were derived with 532nm, 633nm or 1064nm wavelengths of light (table 1). Additional data was found on pig bladder properties at multiple wavelengths [37] and is represented in table 2.

Table 1: Optical parameters of human bladder tissues

Tissue	λ(nm)	Absorption μ_a (cm^{-1})	Scattering μ_s (cm^{-1})	Reference
Whole	532	0.27-0.71	1.28-3.30	[36]
Whole	633	0.28-0.76	2.5-6.37	[36]
Integral	633	1.4	88	[28]
Integral	1064	0.4	116	[38]
Mucous	1064	0.7	75	[38]
Wall	1064	0.9	54.3	[38]

Table 2: Optical parameters of pig bladder tissues

λ(nm)	Absorption μ_a (cm^{-1})	Scattering μ_s (cm^{-1})	Reference
458	1.3	255	[37]
488	1.4	248	
514	1.8	240	
532	3.5	277	
630	0.57	214	
630	0.99	258	

As a starting point, transmission, reflectance and absorbance properties of bladder tissue, as well as the respective coefficients, were required for the basis of the 3D model. The literature review, however, only provided data for a limited selection of wavelengths and for a limited tissue types. As the majority of early BC is present in the mucosa and sub-mucosa layers of bladder and laser diagnostics devices mainly penetrating along their depth, data for these layers was of specific importance. Additionally, for the purposes of the model, coefficients at wavelengths matching biomarkers of interest were required. These biomarkers (particularly collagen, elastin, NADH and FAD) have excitation wavelengths between 260-450 nm and emission wavelengths between 420-530 nm [39].

3.2 3D model

Due to the complex structural nature of the urinary bladder tissue, for the purposes of the theoretical modelling described in this paper, we constructed a simplified dual layer model (mucosa and muscle).

Figure 2a displays the side view of the constructed model, while figure 2b displays the same model in three dimensions. As is evident from figure 2, the diagnostic depth into the tissue is around 1-1.3 mm.

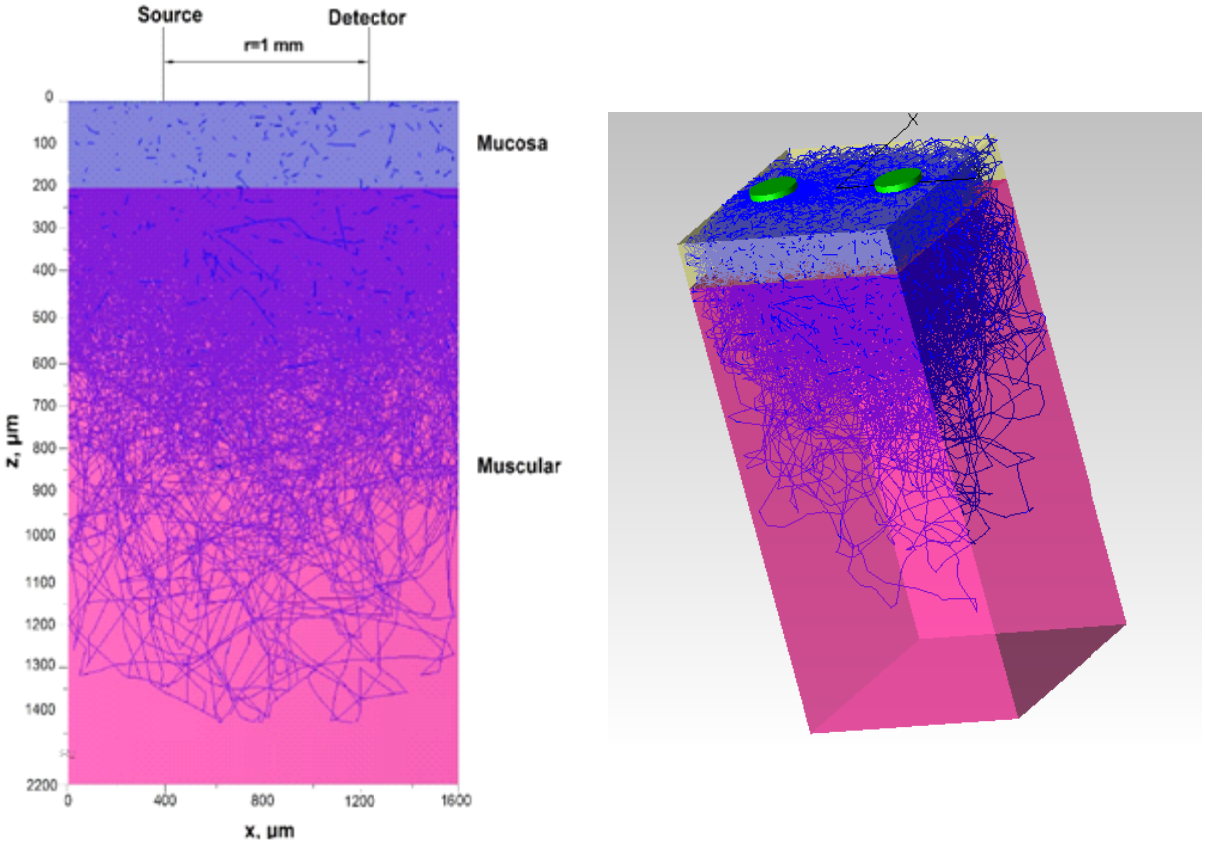

a b

Figure 2. (a) Side view of 3D model. Source, detector and the tissue layers are labelled. The lines indicate the passage of individual photons through the tissue. Darker lines indicate the photons which are heading directly towards the visible flat surface. (b) Full 3D view of model represented in figure 2a. Source and detector are represented by green circles.

3.3 Measured and modelled fluorescence

The results of experimental urinary bladder fluorescence at 365 nm excitation were compared to a simulated cure produced using the 3D model (displayed in figure 3). This simulation incorporates both NADH and collagen presence in the tissue.

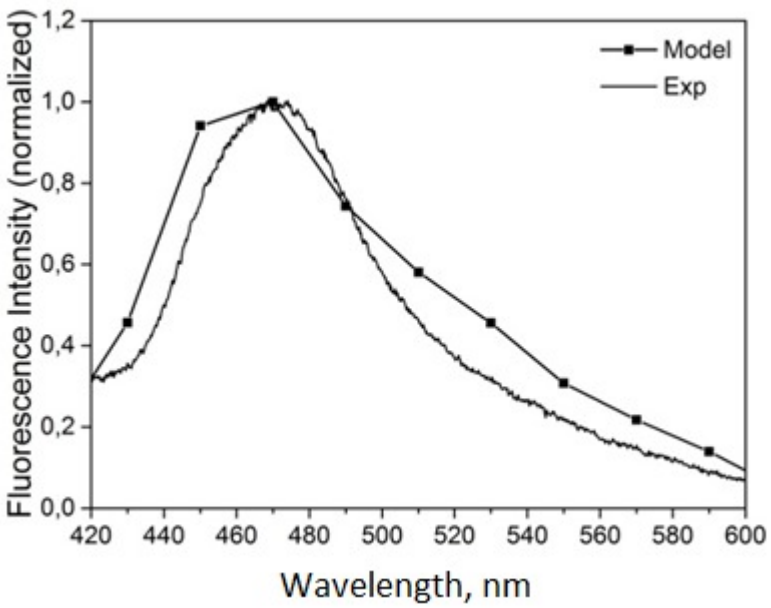

Figure 3. Comparison of experimental and model based spectra, calculated using the Monte-Carlo method. Model simulates presence of NADH and collagen.

With the model, simulated fluorescence spectra can be produced. Upon comparison, we can see a good consistency of the model and experimentally obtained spectra (figure 3). More interesting is the experimental signal in the 510 – 570 nm range. This difference may be characterised by the presence of unaccounted for fluorophores (such as FAD) within the real tissue. Additionally, other absorbing chromophores may contribute to the modification of the experimentally obtained spectrum. It is however possible to conclude that the shape of the experimentally obtained bladder tissue fluorescence spectrum is heavily influenced by the fluorescence of present NADH and collagen.

3.4 Future prospects

As presented above, the described model is capable of simulating the tissue fluorescence of healthy urinary bladder. With the inclusion of simulated parameters for tissue components known to heavily affect light passage such as FAD, the model can be further improved to provide a more accurate representation of living tissue. There is particular scope for improving the model outcome by calculating the optical properties of specific tissue of interest (pig urinary bladder in the case of this study). The procedure to this is relatively simple but would require specialised equipment. Before calculating transport coefficients, a spectrometer with an integrating sphere attachment capable of detecting diffuse reflectance is required. Samples would have to be taken from whole tissue, mucosa and muscle, before being measured for transmission, absorption and diffuse reflectance. These values can then be employed to calculate the required transport coefficients.

For the calculation of the transport coefficients μ_s and μ_a based on the experimetnal spectrometry data, the inverse adding-doubling methodology may be employed. This can provide the coefficient of absorption and reduced scattering coefficient μ_s' (which is = $\mu_s(1 - g)$). The algorithm relies on the use of diffuse reflectance, absorption and transmission measurements as well the anisotropy factor *g*. For the purpose this particular study, *g* would be taken as 0.9 due to this value being most typical for the majority of biotissues in the visible and near infrared spectral wavelengths [40,41].

The determination of the desired transport coefficients is a multistep process. Step 1 required the use of equations 6 and 7.

$$\frac{\mu_s'}{\mu_a + \mu_s'} = \begin{cases} 1 - \left(\frac{1 - 4R_d - T_t}{1 - T_t}\right)^2, if\ \frac{R_d}{1 - T_t} < 0.1 \\ 1 - \frac{4}{9}\left(\frac{1 - R_d - T_t}{1 - T_t}\right)^2, if\ \frac{R_d}{1 - T_t} \geq 0.1 \end{cases} \quad (6)$$

$$(\mu_a + \mu_s')l = \begin{cases} -\frac{lnT_t \ln(0.05)}{lnR_d}, if\ R_d \leq 0.1 \\ 2^{1+5(R_d + T_t)}, if\ R_d > 0.1 \end{cases} \quad (7)$$

Where R_d is the measured value for diffuse reflectance, T_t is the measured value for total transmission and *l* is the thickness of the tissue [42].

Step 2 uses the initial values of μ_s' and μ_a as a basis for reverse calculation of R_d and T_t, following the methodology described by Prahl (1995).

Step 3 is the final step which uses the iterative Nelder-Mead method [44] as demonstrated in equation 8, to compare the experimental (*exp*) and calculated (*calc*) values of diffuse reflectance (R_d) and total transmission (T_t).

$$\frac{\left|R_d^{exp} - R_d^{calc}\right|}{R_d^{exp}} + \frac{\left|T_t^{exp} - T_t^{calc}\right|}{T_t^{exp}} < 0.001 \quad (8)$$

Such methodology would have to be employed for each individual wavelength of interest to determine the optical properties for the entire measured spectrum. The calculation of experimentally obtained transport coefficients would provide specific and vital data that is either limited or unavailable in current literature, particularly on specific wavelengths of interest based on individual fluorophores present in biotissue.

These very promising and substantial results demonstrate the ability of spectroscopic techniques to provide useful information for disease classification in a non-invasive manner. Although each of the techniques discussed in this article shows great potential as a means of detecting dysplasia in bladder, their combination should allow us to create a comprehensive picture of the biochemical and morphological stages of tissue. Specifically, fluorescence changes of biochemicals such as NADH and collagen will provide details about urinary bladder tissue biochemistry. This model has the potential to greatly aid in optical diagnostics of urinary bladder diseases such as cancer, when used in conjunction with other optical diagnostics tools. Further improving the accuracy of the model as described in this discussion will only increase its potential. Additionally, based on the developed optical model and further computer simulations, the general distribution of light within tissue can be predicted. This can be invaluable in a variety of non-invasive optical methods of investigation, ultimately leading to potential new avenues of modelling and diagnostics.

ACKNOWLEDGEMENTS

This work was supported by the European Community's Seventh Framework Programme (FP7-People-2011-IAPP) under Grant Agreement no. 324370 ABLADE and partially by the state task of the Ministry of Education and Science, Russian Federation, for the State University – Education-Science-Production Complex (basic part, №310).

REFERENCES

[1] Sievert, K.D., Amend, B., Nagele, U., Schilling, D., Bedke, J., Horstmann, M., Hennenlotter, J., Kruck, S., and Stenzl, a, "Economic aspects of bladder cancer: what are the benefits and costs?," World journal of urology 27(3), 295–300 (2009).

[2] Jemal, A., Siegel, R., Ward, E., Hao, Y., Xu, J., and Thun, M.J., "Cancer statistics, 2009.," CA: a cancer journal for clinicians 59(4), 225–49 (2009).

[3] Ramanujam, N., "Fluorescence spectroscopy of neoplastic and non-neoplastic tissues.," Neoplasia (New York, N.Y.) 2(1-2), 89–117 (2000).

[4] Palmer, S., Sokolovski, S.G., Rafailov, E., and Nabi, G., "Technologic Developments in the Field of Photonics for the Detection of Urinary Bladder Cancer.," Clinical genitourinary cancer 11(4), 390–6 (2013).

[5] Karaoglu, I., van der Heijden, A.G., and Witjes, J.A., "The role of urine markers, white light cystoscopy and fluorescence cystoscopy in recurrence, progression and follow-up of non-muscle invasive bladder cancer.," World journal of urology (2013).

[6] Brausi, M., Collette, L., Kurth, K., Meijden, A.P. Van Der, Oosterlinck, W., Witjes, J.A., Newling, D., Bouf, C., Sylvester, R.J., et al., "European Urology Variability in the Recurrence Rate at First Follow-up Cystoscopy after TUR in Stage Ta T1 Transitional Cell Carcinoma of the Bladder : A Combined Analysis of Seven EORTC Studies," European urology 41, 523 – 531 (2002).

[7] Jocham, D., Witjes, F., Wagner, S., Zeylemaker, B., van Moorselaar, J., Grimm, M.-O., Muschter, R., Popken, G., König, F., et al., "Improved detection and treatment of bladder cancer using hexaminolevulinate imaging: a prospective, phase III multicenter study.," The Journal of urology 174(3), 862–6; discussion 866 (2005).

[8] Mowatt, G., N'Dow, J., Vale, L., Nabi, G., Boachie, C., Cook, J. a, Fraser, C., and Griffiths, T.R.L., "Photodynamic diagnosis of bladder cancer compared with white light cystoscopy: Systematic review and meta-analysis.," International journal of technology assessment in health care 27(1), 3–10 (2011).

[9] Draga, R.O.P., Grimbergen, M.C.M., Vijverberg, P.L.M., van Swol, C.F.P., Jonges, T.G.N., Kummer, J.A., and Ruud Bosch, J.L.H., "In vivo bladder cancer diagnosis by high-volume Raman spectroscopy.," Analytical chemistry 82(14), 5993–9 (2010).
[10] Anidjar, M., Ettori, D., Cussenot, O., Meria, P., Desgrandchamps, F., Cortesse, A., Teillac, P., Le Duc, A., and Avrillier, S., "Laser Induced Autofluorescence Diagnosis of Bladder Tumors: Dependence on the Excitation Wavelength," The Journal of Urology 156(5), 1590–1596 (1996).
[11] Koenig, F., McGovern, F.J., Althausen, A.F., Deutsch, T.F., and Schomacker, K.T., "Laser Induced Autofluorescence Diagnosis of Bladder Cancer," The Journal of Urology 156(5), 1597–1601 (1996).
[12] Georgakoudi, I., Jacobson, B., and Müller, M., "NAD (P) H and collagen as in vivo quantitative fluorescent biomarkers of epithelial precancerous changes," Cancer research 62, 682–687 (2002).
[13] Walsh, A., Cook, R.S., Rexer, B., Arteaga, C.L., and Skala, M.C., "Optical imaging of metabolism in HER2 overexpressing breast cancer cells.," Biomedical optics express 3(1), 75–85 (2012).
[14] Akbar, N., Sokolovski, S., Dunaev, A.V., Belch, J.J.F., Rafailov, E., and Khan, F., "In vivo noninvasive measurement of skin autofluorescence biomarkers relate to cardiovascular disease in mice.," Journal of microscopy 255(1), 42–8 (2014).
[15] Ostrander, J.H., McMahon, C.M., Lem, S., Millon, S.R., Brown, J.Q., Seewaldt, V.L., and Ramanujam, N., "Optical redox ratio differentiates breast cancer cell lines based on estrogen receptor status.," Cancer research 70(11), 4759–4766 (2010).
[16] Skala, M.C., Riching, K.M., Gendron-Fitzpatrick, A., Eickhoff, J., Eliceiri, K.W., White, J.G., and Ramanujam, N., "In vivo multiphoton microscopy of NADH and FAD redox states, fluorescence lifetimes, and cellular morphology in precancerous epithelia.," Proceedings of the National Academy of Sciences of the United States of America 104(49), 19494–19499 (2007).
[17] Varone, A., Xylas, J., Quinn, K.P., Pouli, D., Sridharan, G., McLaughlin-Drubin, M.E., Alonzo, C., Lee, K., Münger, K., et al., "Endogenous two-photon fluorescence imaging elucidates metabolic changes related to enhanced glycolysis and glutamine consumption in precancerous epithelial tissues.," Cancer research 74(11), 3067–3075 (2014).
[18] Brancaleon, L., Durkin, A.J., Tu, J.H., Menaker, G., Fallon, J.D., and Kollias, N., "In vivo Fluorescence Spectroscopy of Nonmelanoma Skin Cancer," Photochemistry and Photobiology 73(2), 178–183 (2007).
[19] Aihara, H., Tajiri, H., and Suzuki, T., "Application of autofluorescence endoscopy for colorectal cancer screening: rationale and an update.," Gastroenterology research and practice 2012, 971383 (2012).
[20] De Veld, D.C.G., Witjes, M.J.H., Sterenborg, H.J.C.M., and Roodenburg, J.L.N., "The status of in vivo autofluorescence spectroscopy and imaging for oral oncology.," Oral oncology 41(2), 117–131 (2005).
[21] Pavlova, I., Williams, M., El-Naggar, A., Richards-Kortum, R., and Gillenwater, A., "Understanding the biological basis of autofluorescence imaging for oral cancer detection: high-resolution fluorescence microscopy in viable tissue.," Clinical cancer research : an official journal of the American Association for Cancer Research 14(8), 2396–404 (2008).
[22] Zheng, W., Lau, W., Cheng, C., Soo, K.C., and Olivo, M., "Optimal excitation-emission wavelengths for autofluorescence diagnosis of bladder tumors.," International journal of cancer. Journal international du cancer 104(4), 477–481 (2003).
[23] Bigio, I.J., and Mourant, J.R., "Ultraviolet and visible spectroscopies for tissue diagnostics: fluorescence spectroscopy and elastic-scattering spectroscopy.," Physics in medicine and biology 42(5), 803–14 (1997).
[24] Bradley, R.S., and Thorniley, M.S., "A review of attenuation correction techniques for tissue fluorescence.," Journal of the Royal Society, Interface / the Royal Society 3(6), 1–13 (2006).
[25] Tajiri, H., "Autofluorescence endoscopy for the gastrointestinal tract.," Proceedings of the Japan Academy. Series B, Physical and biological sciences 83(8), 248–55 (2007).
[26] Izuishi, K., Tajiri, H., Fujii, T., Boku, N., Ohtsu, A., Ohnishi, T., Ryu, M., Kinoshita, T., and Yoshida, S., "The Histological Basis of Detection of Adenoma and Cancer in the Colon by Autofluorescence Endoscopic Imaging," Endoscopy 31(07), 511–516 (1999).
[27] Vo-Dinh, T., Ed., [Biomedical photonics handbook] , CRC Press, Boca Raton (2010).
[28] Cheong, W., Prahl, S., and Welch, A., "A review of the optical properties of biological tissues," IEEE journal of quantum electronics 26(12), 2166–2185 (1990).
[29] Lurie, K.L., Smith, G.T., Khan, S. a, Liao, J.C., and Ellerbee, A.K., "Three-dimensional, distendable bladder phantom for optical coherence tomography and white light cystoscopy.," Journal of biomedical optics 19(3), 36009 (2014).

[30] Okada, E., and Delpy, D.T., "Near-infrared light propagation in an adult head model. II. Effect of superficial tissue thickness on the sensitivity of the near-infrared spectroscopy signal.," Applied optics 42(16), 2915–22 (2003).
[31] Jacques, S.L., "Optical properties of biological tissues: a review," Physics in Medicine and Biology 58(14), R37–R61 (2013).
[32] Wang, H.-W., Wei, Y.-H., and Guo, H.-W., "Reduced Nicotinamide Adenine Dinucleotide (NADH) Fluorescence for the Detection of Cell Death," Anti-Cancer Agents in Medicinal Chemistry 9(9), 1012–1017 (2009).
[33] A'Amar, O.M., Guillemin, F.H., Begorre, H., and Yvroud, E., "Autofluorescence Spectroscopy of Normal and Pathological Tissues of the Bladder," SPIE proceedings 3197, 41–49 (1997).
[34] Georgakoudi, I., Jacobson, B.C., Van Dam, J., Backman, V., Wallace, M.B., Müller, M.G., Zhang, Q., Badizadegan, K., Sun, D., et al., "Fluorescence, reflectance, and light-scattering spectroscopy for evaluating dysplasia in patients with Barrett's esophagus," Gastroenterology 120(7), 1620–1629 (2001).
[35] Wang, Q., Yang, H., Agrawal, A., Wang, N.S., and Pfefer, T.J., "Measurement of internal tissue optical properties at ultraviolet and visible wavelengths: Development and implementation of a fiberoptic-based system," Optics Express 16(12), 8685 (2008).
[36] Sandell, J., and Zhu, T., "A review of in vivo optical properties of human tissues and its impact on PDT," Journal of biophotonics 4, 773–787 (2011).
[37] Staveren, H. van, "Integrating sphere effect in whole bladder wall photodynamic therapy at violet, green, and red wavelengths," SPIE proceedings 2323, 13–20 (1995).
[38] Muller, G., and Roggan, A., Eds., [Laser-induced interstitial thermotherapy] , SPIE, Bellingham (1995).
[39] Koenig, K., and Schneckenburger, H., "Laser-induced autofluorescence for medical diagnosis.," Journal of fluorescence 4(1), 17–40 (1994).
[40] Bashkatov, A.N., Genina, E.A., Kochubey, V.I., Tuchin, V.V., Chikina, E.E., Knyazev, A.B., and Mareev, O.V., "Optical properties of mucous membrane in the spectral range 350–2000 nm," Optics and Spectroscopy 97(6), 978–983 (2004).
[41] Tuchin, V.V., [Tissue Optics: Light Scattering Methods and Instruments for Medical Diagnosis. SPIE Tutorial Text in Optical Engineering.] , Washington: SPIE Press, 353 (2000).
[42] Prahl, S., Gemert, M. van, and Welch, A., "Determining the optical properties of turbid mediaby using the adding–doubling method," Applied optics (1993).
[43] Prahl, S.., "The adding-doubling method," Optical-thermal response of laser-irradiated tissue (1995).
[44] Bunday, B.D., [Basic optimisation methods] , E. Arnold, Ed., London (1984).